https://doi.org/10.1364/AO.56.009846

Long period fiber grating redefined for biosensing application

SANKHYABRATA BANDYOPADHYAY[1,2], PALAS BISWAS[1], FRANCESCO CHIAVAIOLI[3], TANOY KUMAR DEY[1], NANDINI BASUMALLICK[1],COSIMO TRONO[3], AMBRA GIANNETTI[3], SARA TOMBELLI[3], FRANCESCO BALDINI[3], SOMNATH BANDYOPADHYAY[1*]

[1] *CSIR-Central Glass and Ceramic Research Institute, 196, S. C. Mullick Road, City-Kolkata, PIN-700032, INDIA*
[2] *Academy of Scientific and Innovative Research (AcSIR), CSIR-Central Glass and Ceramic Research Institute, City-Kolkata, PIN-700032, INDIA*
[3]*Institute of Applied Physics "Nello Carrara", CNR-IFAC, Via Madonna del Piano 10, 50019 Sesto Fiorentino, Italy*
**Corresponding author: somnath@cgcri.res.in*

Received XX Month XXXX; revised XX Month, XXXX; accepted XX MonthXXXX; posted XX Month XXXX (Doc. ID XXXXX); published XX Month XXXX

In this paper, investigation on the modeling of LPFG sensors with the aim to provide a more realistic solution for using this family of sensors in bio-sensing is reported. Add-layer sensitivity, i.e. sensitivity of the sensor to an adhered surface has been quantified. A clear understanding about the influence of the thickness of the added analyte layers as well as the change in RI of the said layer on the resonant wavelength of the cladding modes of LPFG has been discussed. Add-layer sensitivity of LPFG sensors around mode transition (MT) and also at turn-around point (TAP) was computed. Numerical results were used successfully to interpret experimental results obtained through model LPFG based bio-sensors.

This template can be used to prepare a research article for submission to *Applied Optics*, JOSA A, or JOSA B. Consult the OSA Author Style Guide for general information about manuscript preparation. © 2015 Optical Society of America

OCIS codes: *(OCIS codes: (060.2310) Fiber optics ; (060.2370) Fiber optics sensors; 280.1415 Biological sensing and sensors.*

1. INTRODUCTION

Usefulness of long period fiber grating (LPFG) based sensors for surrounding refractive index (SRI) sensing is well known [1-4]. The state of the arts may be available in a very recently published review paper where the potential of LPFG based RI sensors in biosensing applications is discussed in detail [5]. Over the years numerous methods have been proposed to increase the sensitivity of the LPFG sensors [6-13]. Sensitivity of these specially tailored LPFG sensors are commendable and design rules show that it is feasible to configure sensors having sensitivity anywhere between 5000 nm/RIU(Refractive Index Unit) to 10000 nm/RIU or even better by an order of magnitude when operated in a small RI range. Most importantly, these LPFG sensors with exceptional performance characteristics have been designed to operate for SRI around 1.33-1.34 RIU because the buffer solutions used around the sensors remain within this range. These high sensitive LPFGs were implemented in label free bio-sensing applications [14-18] where ample information about the bio-molecular interactions taking place around the LPFG could be obtained. There are continuing research efforts to improve upon the sensitivity and to standardize LPFG as a platform for implementing bio-assays.

However though LPFG based RI sensors are capable of producing sufficient information about bio-molecular interactions, one should note that there is still a gap between what we get and what we want. It is evident from the ongoing research in the field of biosensors, that the essence of developing a bio-sensor is to understand the adsorption mechanism of analyte bio-molecules at the receptor sites on the surface of the concerned transducer. The mass uptake of adsorbed bio-molecules, their layer thickness and the local dielectric properties or the refractive index of the layers are considered to be the important measurands. There are quite a good number of established transduction techniques such as quartz crystal microbalance dissipation (QCM-D) [19], surface plasmon resonance (SPR) [20,21] and surface acoustic wave (SAW) based devices [22] which are either able

https://doi.org/10.1364/AO.56.009846

to provide accurate information about the mass accumulation due to adsorption of molecular layers or the dielectric property of the same. Knowing the fact that the adsorption or accumulation of bio-molecules on the surface of the transducer is a complicated process and it is fairly diverse for different species like proteins, toxins, viruses, DNA and bacteria, getting desired results using a single measurement system seems unrealistic. It has been shown that a combination of two complementary techniques is more useful for a complete description of the bio-molecular processes on the surface [23,24]. As for example a combination of SAW/SPR, SAW get hold of the details related with the mass adsorption while SPR provides accurate description of the dielectric properties or RI of the layer and the combination derives precise information about change of thickness of the bio-molecules during the process and also other important parameters [24].

In this circumstances, it may be noted that the approach of using LPFG sensors for bio-sensing applications followed so far, fall short to deal with what exactly is demanded from a biosensor in practice. The constraint is found to be at its fundamental design level.

As discussed before, there are quite a few design available to enhance the response of the LPFG sensors to the RI of the surrounding. For all the cases the ultimate target was to maximize the shift of resonant wavelength (λ_{res}) of the concerned cladding mode of the LPFG as a function of a change of RI of the surrounding medium (n_{SRI}) which was assumed to be extended to infinite distance from the cladding surface. But on the contrary, all the ongoing bio-molecular interaction taking place around the surface of a transducer remain confined within layers of finite thicknesses. Therefore, the sensitivity $d\lambda_{res}/dn_{SRI}$ of a concerned cladding mode which was optimally set for a medium having RI=1.333 next to the cladding surface would immediately be modified with the incorporation of layers, say a standard bio-functional layer and a receptor layer on the fiber surface, which are essential to adsorb analyte molecules. Secondly, the volume RI sensitivity doesn't give any clue to quantify the thickness of adsorbed analyte molecules. Another drawback of the existing model is to optimize the sensor to work and measure RI precisely around 1.333 with a logical assumption that in most of the wet-phase measurements, water or a buffer having RI around 1.333 is generally used around the biosensor. However though, the surrounding environment around a biosensor is mostly around 1.333 but the RI of the layer which of interest i.e. the RI of the layers of analyte bio-molecules is quite different and also vary over a large range depending on the nature and concentration of the molecules[25,26].

In this paper we report our investigation on the modeling of LPFG sensors with an aim to provide a more useful design methodology that can quantify bio-molecular interactions on the surface of the LPFG. Through a detail numerical computation we could provide a clear understanding about the influence of the thickness of the added analyte layers as well as the change in RI of the said layer on the resonant wavelength of the cladding modes of LPFG based sensors. We present our analysis considering LPFG sensors around mode transition (MT) [6] and also at turn-around point (TAP) [2]. Numerical results has been used successfully to interpret experimental results obtained through model LPFG based bio-sensors.

2. DESIGN OF LPFG WITH MULTILAYER OVERLAY

A. Definition of the problem

It has been shown that LPFG volume RI sensitivity can be significantly enhanced if it is designed to operate around mode transition [6,7]. In this case the coupling between the forward propagating core mode and the cladding modes is tailored by deposition of a thin film overlay layer (OL) of RI higher than the cladding material. For a particular thickness of the high RI film, the cladding mode can be made to

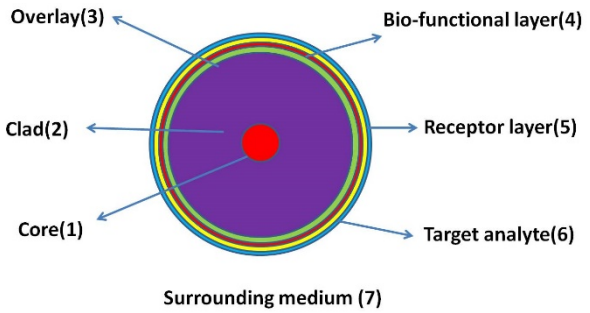

Fig. 1. Proposed multilayered architecture of LPFG for bosensing applications

for transit to its next lower order. During this MT there is a region where the effective index (n_{eff}) of the cladding mode changes linearly with growing thickness of the overlay. If the cladding mode is set to operate around its mode transition, which is generally done by the deposition of an optimum overlay layer thickness (OOT) then the resonant wavelength of the cladding mode changes significantly as a function of the surrounding RI. The slope of the linear part can be made steeper by increasing the RI of the overlay layer. To design a sensor as discussed above, computation of the propagation constants of the modes and subsequently coupled mode analysis is done typically for a four-layer waveguide structure (e.g. core-clad-OL-surrounding medium). The sensitivity (S) of the sensor is generally obtained by recording the shift of the resonant wavelength of the cladding mode as a function of the surrounding RI (i.e. using the parameter $d\lambda_{res}/dn_{SRI}$).

Insufficiency in this design approach may be explained once we consider Fig.1. In this figure, a standard layered structure generally required on the fiber surface to use an LPFG as a biosensor is shown. On the OL, there is another layer of a polymeric material which acts as a bio-functional layer (BFL). In addition to this, a layer generally defined as a receptor layer (RL) of bio-molecules is immobilized on the BFL. The final layer is composed of the molecules of the target analyte (AL). It is apparent from the figure that the LPFG sensor is said to be set for attaching the target analytes only after the suitable receptor layer is immobilized. Therefore, when the cladding mode of interest is already positioned optimally by the deposition of an OOT, it will never be in the same position after deposition of the BFL and the RL. Particularly, for a steeper slope of the MT, deposition of these two layers may completely transit the mode to an insensitive zone before any analyte is tested. Hence, it is necessary to optimize the OL thickness for positioning the cladding mode at highest sensitive linear part taking specific BFL and RL in consideration.

Similar will be the case for LPFG sensors operating at dispersion turn-around-point (TAP) [2,7-9]. The LPFG sensors designed to operate near the TAP of the phase matching curve (PMC) is extremely sensitive to the surrounding. Deposition of BFL and RL alters the phase matching curve and shifts the operating point of the LPFG from the TAP thereby causing a significant reduction

https://doi.org/10.1364/AO.56.009846

in its sensitivity. Therefore, accurately designing a cladding mode that operate near the TAP also demands to take appropriate BFL and RL into consideration during tailoring of the PMC.

It is clear from the above arguments that coupled mode analysis for a multilayered overlay structure on the cladding is a requirement to properly design an LPFG based biosensor that would be able to quantify adsorption of analyte bio-molecules with optimal sensitivity. Secondly, for bio-sensing application, we also propose to redefine the sensitivity to explicitly talk about the sensitivity of the sensor with respect to the thickness of the added layer of analytes and also to the change in the RI of the layer of analytes. Therefore, it will be more appropriate for this case to optimize a sensitivity S_A namely the ad-layer sensitivity which may be defined as

$$S_A = \frac{d\lambda_{res}}{dH_{AL}} + \frac{d\lambda_{res}}{dn_{AL}} \qquad (1)$$

where the first term is the sensitivity of the cladding mode for a change in the layer thickness (H) of the analyte layer (say S_H) and the second term is the sensitivity due to the changes in the layer refractive index (say S_{LRI}). In subsequent sections we present our results for an LPFG with multiple overlay layer operating at mode transition and then for an LPFG operating at the TAP. Ad-layer sensitivity for the respective cases has also been studied.

B. Basic theory

The generalized transfer matrix formulation based on LP modes for a multilayer dielectric waveguide structure given in [23,24] is utilized for modelling LPFG with multilayer overlay deposition .

Transverse Electric field components propagating along the z axis can be given by

$$\psi(r,\theta,\phi) = e^{-j\beta_{\nu,j}z}\psi(r)\Theta(\theta)\Phi(\phi) \qquad \mathbf{(2)}$$

where the radial function $\Psi(r)$of the individual layer can be written as

$$\psi(r) = A_{\nu,j}J_\nu(r\gamma_{\nu,j}) + B_{\nu,j}Y_\nu(r\gamma_{\nu,j}) \;\; \beta_{\nu,j} < k_0 n \qquad \mathbf{(3)}$$

$$\psi(r) = A_{\nu,j}I_\nu(r\gamma_{\nu,j}) + B_{\nu,j}K_\nu(r\gamma_{\nu,j}) \;\; \beta_{\nu,j} > k_0 n \qquad \mathbf{(4)}$$

Where $k_0 = \frac{2\pi}{\lambda}$ is the free space wavelength, n is the refractive index of the layer, β_{vj} is the longitudinal propagation constant of the LP_{vj} mode and $\gamma_{\nu,j} = \sqrt{[k_0^2 n^2 - \beta_{\nu,j}^2]}$ is the magnitude of the transverse wave number. $A_{\nu,j}$ and $B_{\nu,j}$ are the field expansion coefficients determined by the boundary condition of the cylindrical layers. $J_\nu(r\gamma_{\nu,j})$ and $Y_\nu(r\gamma_{\nu,j})$ are the ordinary Bessel function of the first and second kind, while $I_\nu(r\gamma_{\nu,j})$ and $K_\nu(r\gamma_{\nu,j})$ are the modified Bessel function of first and second kind of order ν. The transfer matrix methods have been applied to find out the effective indices of the modes and field expansion coefficients of multi-layer LPFG waveguide structure. Field expansion coefficients of each layer are normalized so that each mode carries the same power P_0.

$$P_0 = \frac{\beta_{0j}}{2\omega\mu_0}\int_0^{2\pi} d\Phi \int_0^{\infty} \psi(r)\psi^*(r) r dr \qquad \mathbf{(5)}$$

After the derivation of field expansion coefficients for each layer coupled mode differential equations are formed. We assumed each of the forward propagating modes have complex amplitude $A(z)$ and neglect backward propagating scattered wave. The generalized coupled mode equations are

$$\sum_{\nu} \frac{dA_{\mu k}}{dz} = -j\sum_{vj=01}^{M} [K_{vj,\mu k}^{t} + K_{vj,\mu k}^{z}] A_{\nu,j}(z) exp(-j(\beta_{vj} - \beta_{\mu k})z) \qquad \mathbf{(6)}$$

for μk= 01,..... M; $K_{vj,\mu k}^{t}$ and $K_{vj,\mu k}^{z}$ are the transverse coupling and longitudinal coupling coefficients between LP_{vj} and $LP_{\mu k}$ modes. It is assumed that $K_{vj,\mu k}^{t} >> K_{vj,\mu k}^{z}$ so only transverse coupling coefficients are considered between the modes. Transverse coupling coefficients has been computed using the equation prescribed in [30]

$$K_{vj,\mu k}^{t} = \int_{\Phi=0}^{2\pi} d\Phi \int_{r=0}^{\infty} \Delta\varepsilon\psi_{vj}(r)\psi_{\mu k}(r) r dr \qquad \mathbf{(7)}$$

Where ψ_{vj} and $\psi_{\mu k}$ are the transverse field components of LP_{vj} and $LP_{\mu k}$ modes. $\Delta\varepsilon$ is the permittivity variation, for this particular waveguide problem. It is defined as 2nΔn, where Δn is the change in refractive index of the core during grating writing.

Resonance wavelength of a clad mode has been computed using the phase matching condition given as $\beta_{01} - \beta_{0\nu} = \frac{2\pi}{\Lambda}$ which in turn gives the resonance wavelength of each clad mode as $\lambda_{reso,m} = (n_{co}^{eff} - n_{cl,m}^{eff})\Lambda$ where n_{co}^{eff} is the effective index of the core mode and $n_{cl,m}^{eff}$ are the effective indices of m^{th} order clad mode respectively.

C. Design analysis of LPFG at mode transition

In this section we describe our numerical results through quantitative analysis of an LPFG having multiple overlay layer operating near mode transition. To accomplish that we have numerically solved set of coupled mode equations as given in Eq. 5 to investigate the coupling between a fundamental core mode and co-propagating cladding modes for a seven layer waveguide structure (e.g. core-clad-OL-BFL-RL-AL-surrounding) as given in Fig. 1. We considered fiber parameters for SMF-28, BFL of thickness 5nm with RI=1.54 and RL with RI=1.6. We consider the BFL is a layer of polymer e.g. Eudragit L-100. The RL is a layer of protein molecules which acts as receptors. The RI of the OL can have a wide range depending on the choice of the material. We analyze the response characteristics of LP_{07} cladding mode of LPFG sensor for two different OL materials, one with RI=1.7 and

https://doi.org/10.1364/AO.56.009846

the other with RI=2.0. The basis for this is simply because the authors have already carried out experiments [..] where a Ti doped SiO_2 layer having RI ~1.7 was deposited on the fiber using sol-gel

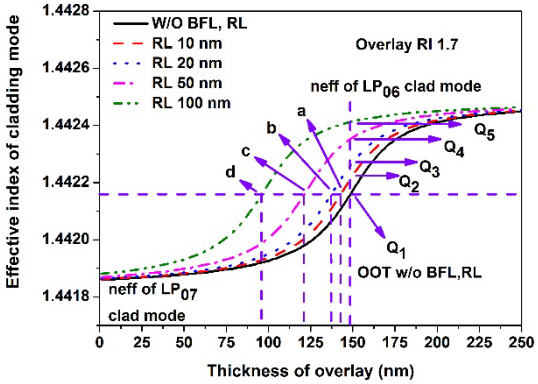

Fig. 2. Variation of effective index of cladding mode with deposition of overlay RI of 1.7, considering a fixed BFL and different thicknesses of RL.

technique. On the other hand a TiO_2 layer can have a RI ~2.0. The analysis however may be carried out for any other OL material. We have considered water (RI=1.333) in the surrounding.

Fig. 2 shows the variation of effective index of LP_{07} cladding mode as a function of OL considering varying thicknesses of RL. The figure clearly shows how the thickness of the OL (RI=1.7) which is crucial to transit LP_{07} cladding mode to its next lower order mode i.e. the LP_{06} mode is influenced by the thickness of RL (for 10nm, 20nm, 50nm and 100 nm in this simulation). Undeniably in real application, the thickness of the RL will always vary depending on the choice of receptor bio-molecules. For all the cases we consider the BFL to be 5nm. The figure also clearly shows the change in the operating point of a cladding mode with varying RL. As per the present example, the figure shows that for an OOT of ~150nm and without any BFL and RL the LP_{07} cladding mode can be positioned at the midpoint (say Q1) of the linear zone of the MT curve where the volume RI sensitivity is maximum. The operating point successively changes to Q2, Q3 and ultimately to Q5 for deposition of RL of different thicknesses as considered in our analysis. It is apparent that deposition of BFL and RL increases the effective index of the cladding mode and as a result the operating point gradually moves out of the linear high sensitive zone. The shift of the best operating point as a function of RL would be faster for a thin film overlay with higher RI. We have computed the volume RI sensitivity of the cladding mode at the highest

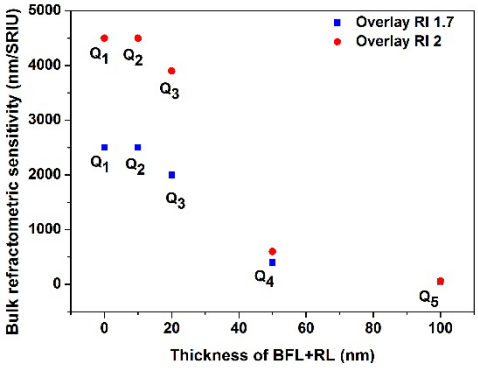

Fig. 3. Numerically computed sensitivity of LP_{07} cladding mode of LPFG at various operating points with overlay RI 1.7 and 2.

sensitive point Q1 and also for respective shifted points to understand how the sensitivity is affected upon deposition of these layers which may vary in case to case. We have computed the sensitivities for two different thin film overlays (OL) with RI=1.7 and also for RI=2.0. The result is shown in Fig. 3. For RI=1.7, at Q1, the volume RI sensitivity around 1.333 was found to be ~ 2500 nm/RIU and it drops down to < 50 nm/RIU at Q5 for comparatively thicker layer of RL. The situation is much sever for OL with RI=2 where the sensitivity comes down from ~4500 nm/RIU (at Q1) to ~50 nm/RIU (at Q5).

Equipped with the model with multiple overlay layers we could estimate the shift of the resonant wavelength of the cladding mode with the growth of adsorbed analyte biomolecules on the RL. Fig. 4 illustrates the shift of resonant wavelength of LP_{07} cladding mode as a function of adhesion of AL in nm for the similar values of BFL and RL as considered earlier. As observed

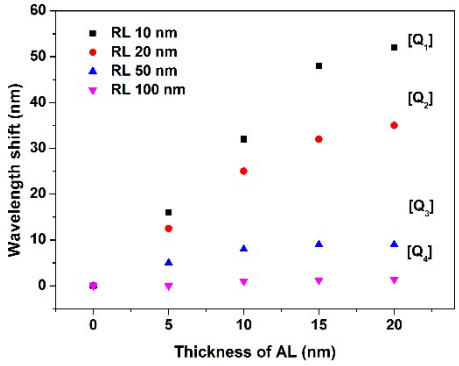

Fig.4. Computed add layer sensitivity (S_H) of LP_{07} cladding mode at different operating point

earlier for the case of volume RI sensitivity the AD-layer sensitivity also is significantly influenced for varying overlay layers of bio-molecules (RL). Redefined sensitivity S_H and S_{LRI} have been computed numerically for each of the operating point and are given in Table.1. It is therefore apparent that the original sensitivity can be maintained if the OOT is judiciously chosen at the design phase for a specific anticipated BFL and RL. We have computed the required OOT for different

https://doi.org/10.1364/AO.56.009846

Table.1. Estimated sensitivity of LP_{07} cladding mode (volume and Add layer sensitivity (S_H,S_{LRI})) with different thickness of receptor layer

LPFG sensitivity near MT (OL RI 1.7) with or without BFL and RL	Bulk RI sensitivity (nm/SRIU)	Ad layer sensitivity S_H(nm/nm attachment of AL)	Ad layer sensitivity S_{LRI} (nm/Unit surface RI)
Without BFL and RL	~2500	~4.7	~168
RL=10 nm	~2500	~4.7	~168
RL=20 nm	~2000	~3.2	~135
RL=50 nm	~400	~0.5	~28
RL=100 nm	~50	~0.02	~NA

thicknesses of BFL and RL for two different RI of the OL (points indicated with a, b, c, d in the graph in Fig. 2. Table 2 describes the results. It is clear that necessary adjustment of OOT is substantial when one has to deal with a comparatively thicker layer of receptor molecules in practice.

Table.2. Required OOT for cladding mode to achieve maximum sensitivity with different thickness of RL

Thickness of RL	Required OOT for OL RI 1.7 (nm)	Required OOT for OL RI 2 (nm)
Without RL	~150	69
RL=10 nm	~143.5	65
RL=20 nm	~137	61
RL=50 nm	~118	53.5
RL=100 nm	~90	41

D. Analysis of LPFG at TAP

In this section we extended our investigation to understand the design issues of another family of high sensitive LPFG sensor commonly known as TAP-LPFG. RI sensitivity of a cladding mode can be significantly enhanced when the cladding mode is designed to operate near the TAP of its PMC. RI sensors configured based on this methodology has also been widely used for biosensing applications [5]. In general there are two distinct methodologies based on which TAP-LPFGs are used for refractive index sensing. It is known that the resonance between the core mode and a specific higher order cladding mode at TAP of PMC produces a single broadband attenuation around the TAP. As per the first methodology, an LPG with a single attenuation band centred around the TAP is designed in away so that any change of surrounding index modifies the peak attenuation at the resonant wavelength without altering the resonant wavelength. However, the methodology which is used more frequently is to design a TAP-LPG which produce a single attenuation band in presence of air in the surrounding. The same LPFG when immersed in an environment having refractive index higher than that of air (say water or any buffer solution having its RI very near to that of water), the single wide band resonant peak splits into two in either side of the resonant wavelength at the TAP. Shift of either of these two resonant wavelengths or both are usually monitored for subsequent change in surrounding RI. It was shown that closer the split resonant band with respect to the TAP higher is the sensitivity [2]. A post fabrication fine tuning of the PMC was found to be a useful technique to position the split resonant band in close neighbourhood of the TAP [9].

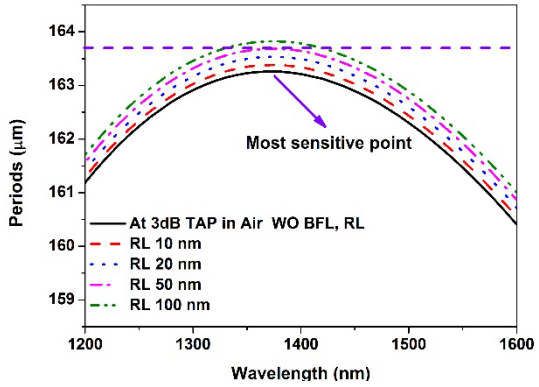

Fig.5. Computed phase plot of $LP_{0,12}$ cladding mode in air with consideration of different thickness of RL.

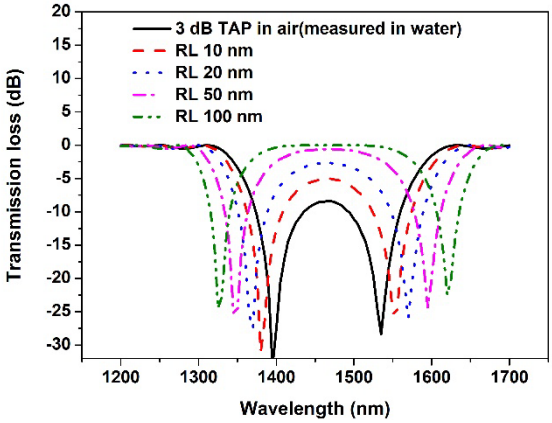

Fig.6. Numerically computed spectrum of $LP_{0,12}$ cladding mode with consideration different thickness values of RL with surrounding medium as water.

In this section we investigate the response of a higher order cladding mode working near the TAP of its PMC considering multiple layered structure as described in Fig.1. In this case the thin film overlay layer OL used to position the cladding mode at MT was not considered. In this example we considered the parameters of a standard single mode fiber SMF-28. Firstly we simulated an LPFG by solving the coupled mode equations for a three layer architecture (say core-clad-surrounding) with a period ~163.7 nm to have the $LP_{0,12}$ cladding mode at the TAP of its PMC considering RI=1 in the surrounding. The separation between the split resonant band for water (RI=1.333) in the surrounding was found to be ~250nm. The PMC was then tuned by gradually reducing the cladding diameter to ~123 μm to narrow down the separation to ~ 130nm with a significantly high bulk RI sensitivity of ~1788 nm/RIU for a RI change of the surrounding in the range from 1.33 to 1.34. Now the designed PMC will certainly shift by deposition of layers polymers and receptor layers. To quantify the same we carried out coupled mode analysis for a five layer waveguide structure (e.g. core-clad-BFL-RL-surrounding(RI=1.0)). Shift of the PMC for the

https://doi.org/10.1364/AO.56.009846

$LP_{0,12}$ cladding mode from its original location for different RL is shown in Fig.5. Corresponding spectra of $LP_{0,12}$ cladding mode with a dual resonant band (surrounding RI=1.333) have also been computed for increasing thickness of RL and are shown in Fig. 6. We subsequently computed the volume RI sensitivity and also the Ad-layer sensitivity for each of the cases and the results are tabulated in Table 3. It is apparent that the performance of an LPFG optimally designed to work around TAP using a three layer model, drops significantly when is used for bio-sensing application with multiple layers on the fiber surface. It is therefore evident that designing the sensor to perform around its optimum sensitivity, a clear understanding of the behaviour of the respective cladding modes as a function of deposition of multiple layers is desired where the coupled mode analysis considering multiple overlay structure helps.

3. INTERPRETATION OF EXPERIMENTAL RESULTS AND DISCUSSION

The aim of this section is to exploit the concept of add-layer sensitivity of LPFG sensors to interpret the mean layer thickness of the adsorbed layer from the shift of the resonant wavelength of a cladding mode as obtained experimentally from two model bioassays [16,17]. In one case the authors have performed experiments with a TAP-LPFG considering a higher order $LP_{0,12}$ cladding mode [16]. On the second model the $LP_{0,7}$ cladding mode was designed to operate around the linear

Table.3. Bulk RI sensitivity and add layer sensitivity of $LP_{0,12}$ cladding mode with different thickness of RL

Sensitivity of cladding mode of LPFG near TAP	Bulk RI sensitivity (nm/SRIU) [Dual resonance band sensitivity]	Ad layer sensitivity S_H(nm/nm attachment of AL)	Ad layer sensitivity S_{LRI} (nm/surface change in RI)
Without BFL and RL	~1788	1.93	~120
RL=10 nm	~1560	1.78	~102
RL=20 nm	~1105	0.93	~78
RL=50 nm	~876	0.61	~60
RL=100 nm	~541	0.22	~34

region of its mode transition. We used a sol-gel derived Ti-doped SiO_2 layer (RI ~1.7) as a thin film overlay for positioning the LP_{07} cladding mode in the high sensitive linear zone of its MT curve [17]. Subsequently antibody-antigen binding kinetics for specific analyte concentrations was determined. The preparation of the bio-assay consisted of the following steps: i) deposition of Eudragit-L100 as a bio-functional layer and activation of –COOH groups by cross-linking chemistry (EDC and NHS), ii) covalent immobilization of mouse IgG (1000 mg/L), iii) washing with phosphate buffered saline (PBS) to remove the un-reacted IgG. The response of the sensor was then recorded for the antigen binding steps, with increasing concentrations of anti-mouse IgG ranging from 1 mg/L to 100 mg/L.

We will first discuss the results obtained using the TAP-LPFG. First a three layer model (core-clad-surrounding) was used to position the $LP_{0,12}$ cladding mode as done during the sensor fabrication. The surrounding material was considered to be PBS (RI=1.334). As described in section 2, to quantify the thickness of a deposited layer with known RI we have to compute the sensitivity of the sensor for adhesion of a layer i.e. S_H. We start with deposition of a layer of Eudragit L-100. Being a polymer, we assumed that a layer of material with RI=1.5 was deposited and for which S_H of the sensor was found to be ~ 1.27 nm/nm (i.e. nanometer of wavelength shift per nanometer of deposited layer) by carrying out coupled mode analysis of a four layer model (core-clad-Eudragit-PBS). The measured wavelength shift after deposition of Eudragit was ~5.1 nm. Therefore, the estimated thickness of Eudragit layer was found to be ~4.1 nm. The next layer of our experiment was a layer of mouse-IgG having a concentration of 1000mg/L which acts as a receptor layer. We considered the average RI of the closely packed IgG molecules to be 1.46 [23-25]. It is understood that the RI of a layer of IgG molecules may vary over a wide range (1.435-1.465) depending on the water content of the layer. As in our experiment a very high concentration of IgG was used, considering the average RI on the higher side seems to be a valid assumption. With this assumption, we recalculated S_H considering a five layer waveguide structure (core-clad-Eudragit-IgG-PBS) which was found to be ~0.76 nm/nm. With this sensitivity, the estimated thickness of the IgG layer was found to be ~5.44nm from the recorded wavelength shift. Estimation of added layer thickness on the receptor layer for different concentration of anti-mouse-IgG was computed with the same S_H. This is also a valid assumption considering the fact that the anti-mouse IgG and mouse IgG have similar molecular characteristics. The thicknesses estimated from the recorded wavelength shifts for the concentrations 1mg/L, 10mg/L and 100mg/L were found to be ~0.835nm, ~1.74nm and ~4.14nm respectively.

To interpret the results obtained in the other experiment [17] where an $LP_{0,7}$ cladding mode was designed to operate near mode transition, we compute the add layer sensitivity (S_H) for the cladding mode following similar methodology as described above. In our second experiment, the $LP_{0,7}$ cladding mode was designed in such a way that after deposition of Eudragit and a layer of mouse IgG molecules as receptor, the cladding mode is positioned in most sensitive linear region point for detection of target analyte. To estimate thicknesses of anti-mouse IgG (the analyte) deposited on the sensor surface for exposing the sensor in analyte solution with different concentration we computed add-layer sensitivity (S_H) considering the multilayered waveguide structure applicable for the present case (i.e. core-clad-OL-Eudragit-mouse IgG- antimouse IgG-PBS). The computed S_H in the linear region of the MT curve was found to be ~1.3 (nm/nm). The thicknesses estimated from the recorded wavelength shifts for the concentrations 0.1mg/L, 1mg/L and 10mg/L were found to be ~0.338nm, ~0.569 nm and ~2.66nm respectively. It is interesting to note that the order of magnitude of the thicknesses estimated using the multilayered model closely match with the results obtained elsewhere [23]. This is to note that thickness estimated for very low concentration (say 0.1 mg/L) of analytes could not be corroborated due to non availability of measured data in the literature.

4. DISCUSSIONS

It is therefore established that LPFG sensors, if modeled suitably, can realistically measure the thickness of the deposited layer of

https://doi.org/10.1364/AO.56.009846

molecules, even at sub-nanometer level, in terms of the shift of resonant wavelength of its cladding modes. This is certainly an important measureand to comprehend adsorbed mass of bio-molecules deposited on the sensors surface which subsequently provides ample information about the reaction kinetics in the field of bio-sensing. The thicknesses have been estimated based on the assumption that the analyte bio-molecules forms a closely packed layer on the surface of the LPFG with an average RI which is characteristic to those specific molecules. With this assumption, computation of S_H seems to be sufficient to describe the process. As it is valid for other standard measurement techniques like SAW, QCM-D, for LPFG also the level of precision with which the thicknesses can be estimated depends on the accuracy of the average RI of the thin layers of the bio-molecules [23,24]. A standard database about the dielectric properties and the density of the concerned layers for specific group of molecules should be made available either by ellipsometry or by an SPR based measurement. The accuracy of wavelength measurement for LPFG should not be a constraint with available high precision instruments.

For very low concentration of analyte molecules the proposition discussed above may be argued. However though, it is understandable that for a surface saturated with receptors, the adsorbed mass of analyte is directly correlated with the concentration of the analyte molecules in the solution. Yet, at very low analyte concentration, the adsorption of analyte molecules on the receptor surface may be spares enough so that interpretation of adsorbed mass in terms of thickness may be questionable. In that case quantification of the adsorbed mass may be done in terms of change in local RI of the receptor layer with an assumption that adsorbed thickness of analyte is negligible. Therefore, add-layer sensitivity S_{LRI} will be useful to estimate the adsorbed mass.

The specific concern with the LPFG sensors having been resolved, the next immediate task would be to design LPFG sensors with high add-layer sensitivity so that it may compete with other surface sensitive techniques used in label free bio-sensing. Recently published interesting approaches used for enhancement of volume RI sensitivities, [10,13] can easily be recast in the proposed multilayered architecture to optimize the ad-layer sensitivity. Other methodologies may also be explored to enhance the add-layer sensitivity [28]. The basic modeling methodology proposed will also be useful to redefine the sensitivity of symmetric and asymmetric cladding modes of un-tilted and tilted fiber Bragg gratings, [29,30] to employ these sensors for chemical and biological recognition elements on the surface of the fiber. Moreover, use of nano-structured coatings of specialty materials on the fiber surfaces has already turn out to be another valuable means to develop chemical and biosensors [31]. The nano-structured coatings, depending on the nature of the coatings say thickness, average RI, induces significant changes in the coupling conditions of the evanescent field of the cladding modes with the surrounding. Here also quantifying add-layer sensitivity and subsequent enhancement of the same through optimization of those layers of nano-structured materials is a necessity to use these devices for detection of biological and chemical recognition elements on the surface of the sensor.

5. CONCLUSION

Add-layer sensing characteristics of an LPFG sensor has been investigated in this paper. The proposed modeling methodology could successfully interpret experimental results. It has been shown that this sensor is able to quantify the adsorbed layer of bio-molecules either in terms of its thickness or the RI. Suitably designed LPFG sensors can therefore provide another platform that can complement other established surface sensitive sensing techniques for label free bio-sensing, subsequently to produce complete description of the chemical and bio-molecular reaction kinetics taking place around the surface of the sensor. There are ample scope to practically enhance the add-layer sensitivity of LPFG sensor with the available state of the art of LPFG fabrication and of highly accurate layer deposition methods on the surface of the LPFG. Therefore, monitoring the growth of bio-molecules on the surface in real time will also be a possibility.

References

1. H. J. Patrick, A. D. Kersey, and F. Bucholtz, "Analysis of the Response of Long Period Fiber Gratings to External Index of Refraction," *J. Lightw. Technol.,vol. 16,* No. 9 pp. 1606-1612, 1998
2. Xuewen Shu, Lin Zhang, Ian Bennion, "Sensitivity Characteristics of Long-Period Fiber Gratings" Journal of Lightwave Technology, vol. 20, no. 2, pp. 255-266, February 2002.
3. Yahei Koyamada, "Numerical Analysis of Core-Mode to Radiation-Mode Coupling in Long-Period Fiber Gratings**",** *IEEE Photonics Technology Letters*, Vol. 13, No. 4, pp. 308-310, April 2001.
4. R Hou, Z Ghassemlooy, A Hassan, C Lu and K. P. Dowker, "Modelling of long period fiber grating response to refractive index higher than that of cladding*," Meas. Sci. Technol*. Vol.-12, pp. 1709-1713, September, 2001.
5. Francesco Chiavaioli, Carlos A. J. Gouveia, Pedro A. S. Jorge, and Francesco Baldini, "Towards a Uniform Metrological Assessment of Grating-Based Optical Fiber Sensors: From Refractometers to Biosensors," Biosensors, Vol-7, Issue No. - 2, June, 2017
6. N. D. Rees, S. W. James, R. P. Tatam, and G. J. Ashwell, "Optical fiber long-period gratings with Langmuir-Blodgett thin-film overlays," Opt. Lett.,**27**, 686–688, (2002).
7. Ignacio Del Villar, Miguel Achaerandio, Ignacio R. Matías, and Francisco J. Arregui, "Optimization of sensitivity in Long Period Fiber Gratings with overlay deposition", *Opt.Exp.vol. 13*, No. 1, pp. 56-68, 2005.
8. P. Pilla, C. Trono, F. Baldini, F. Chiavaioli, M. Giordano and A. Cusano, "Giant sensitivity of long period gratings in transition mode near the dispersion turning point: an integrated design approach", Opt. Lett., vol. 37, no. 19, pp. 4152-4154, Jan. 2012.
9. Palas Biswas, Nandini Basumallick, Sankhyabrata Bandyopadhyay, Kamal Dasgupta, Ajay Ghosh, and Somnath Bandyopadhyay, "Sensitivity Enhancement of Turn-Around-

https://doi.org/10.1364/AO.56.009846

Point Long Period Gratings By Tuning Initial Coupling Condition" IEEE Sensor Journal, vol.15 no.2 pp. 1240-1245. 2015.

10. I. D. Villar, "Ultrahigh-sensitivity sensors based on thin-film coated long period gratings with reduced diameter, in transition mode and near the dispersion turning point", Opt. Exp., vol. 23, no. 7, pp. 8389-8398, Apr. 2015.

11. Jianchun Yang, Lang Zhou, Jing Huang, Chuanyi Tao, Xueming Li , Weimin Chen "Sensitivity enhancing of transition mode long-period fiber grating as methane sensor using high refractive index polycarbonate/cryptophane A overlay deposition" Sensor and Actuator B, 207 (2015) 477–480.

12. L. Coelho, D. Viegas, J. L. Santos, J. M. M. M. deAlmeid, "Characterization of zinc oxide coated optical fiber long period gratings with improved refractive index sensing properties", Sensor Actuat B-Chem., vol. 223, pp. 45-51,Feb. 2016.

13. M. Smietana, M. Koba, P. Mikulic, and W. J. Bock, "Combined Plasma-Based Fiber Etching and Diamond-Like Carbon Nano-overlay Deposition for Enhancing Sensitivity of Long-Period Gratings", J. Lightwave Technol., vol. 34, no. 19, pp. 4615-4619, Oct. 2016.

14. Xianfeng Chen, Lin Zhang, Kaiming Zhou, Edward Davies, Kate Sugden, Ian Bennion, Marcus Hughes, and Anna Hine, " Real-time detection of DNA interactions with long period fiber-grating-based biosensor " *Optics Letters* / Vol. 32, No. 17 / sept, 2007. pp 2541-2543.

15. P. Pilla, P. Foglia Manzillo, V. Malachovska, A. Buosciolo, S. Campopiano, A. Cutolo, L. Ambrosio, M. Giordano, A. Cusano "Long period grating working in transition mode as promising technological platform for label-freebiosensing" 26 October 2009 / Vol. 17, No. 22 / Optics Express 20039-20050.

16. F. Chiavaioli, P. Biswas, C. Trono, S. Bandyopadhyay, A. Giannetti, S. Tombelli, N. Basumallick, K. Dasgupta and F. Baldini, "Towards sensitive label-free immune-sensing by means of turn-around point long period fiber gratings," *Biosens. Bioelectron., vol. 60*, pp. 305–310, 2014.

17. Francesco Chiavaioli, Palas Biswas,, Cosimo Trono, Sunirmal Jana, Somnath Bandyopadhyay, Nandini Basumallick, Ambra Giannetti, Sara Tombelli, Susanta Bera, Aparajita Mallick, and Francesco Baldini, "Sol-gel based titania-silica thin film overlay for long period fiber grating-based biosensors" *Analytical chemistry,* vol.87, pp.12024-12031, November. 2015.

18. Ewa Brzozowska, Marcin Koba, Mateusz Śmietana, Sabina Górska, Monika Janik, Andrzej Gamian and Wojtek J. Bock, "Label-free Gram-negative bacteria detection using bacteriophage-adhesin-coated long-period gratings," BIOMEDICAL OPTICS EXPRESS, Vol. 7, No. 3, pp 829-840 , 2016.

19. C. Galli Marxer, M. Collaud Coen, L.. Schlapbach, "Study of adsorption and viscoelastic properties of proteins with a quartz crystal microbalance by measuring the oscillation amplitude," *J. Colloid Interface Sci.* Vol. 261, Issue 2, pp. 291-298, 2003.

20. P. Kvasnicka and J. Homola" Optical sensors based on spectroscopy of localized surface plasmons on metallic nanoparticles: Sensitivity considerations" Biointer*phases*3(3) September 2008, pp (FD4 - FD11).

21. Xiaowei Guo, " Surface plasmon resonance based biosensor technique: A review," J. Biophotonics, Vol. 5, issue. 7, pp. 483-501, 2012.

22. E. Gizeli, "Acoustic transducer" Chapter-7, pp. 176-206 in *Biomolecular Sensors*, edited by E. Gizeli and C. R. Lowe, Taylor and Francis, London, 2002

23. Cheng Zhou, Jean-Michel Friedt, Angelina Angelova,Kang-HoonChoi, Wim Laureyn, Filip Frederix, Laurent A. Francis, Andrew Campitelli, Yves Engel borghs, and Gustaaf Borghs "Human Immunoglobulin Adsorption Investigated by Meansof Quartz Crystal Microbalance Dissipation, Atomic Force Microscopy, Surface Acoustic Wave, and Surface Plasmon Resonance Techniques" Langmuir, vol.20, no.14, pp.5870-5878, 2004.

24. J. M Friedt, L. Francis, G. Reekmans, R. De Palma, A. Campitelli and U. B. Sleytr, " Simultaneous surface acoustic wave and surface plasmon resonance," J. of Appl. Phys., Vol. 95, No. 4, pp. 1677-1680, 2004

25. N.J.Geddes, A.S.Martin , F.Caruso, R.S. Urquhart, D.N.Furlong, J.R.Sambles, K.A.Than, J.A.Edger "Immobilisation of IgG onto gold surfaces and its interaction with anti-IgG studied by surface plasmon resonance" Journal of Immunological methods, 175, 1994, 149-160.

26. E. Anemogiannis, E. N. Glytsis, and T. K. Gaylord," Transmission Characteristics of Long-Period Fiber Gratings Having Arbitrary Azimuthal/Radial Refractive Index Variations," *J. Lightw. Technol., vol. 21*, No. 1, pp. 218-227, 2003.

27. Katsumi Morishita, "Numerical Analysis of Pulse Broadening in Graded Index Optical Fibers" *IEEE T. Microw Theory. vol. 29*, No. 4, pp. 348-352, 1981.

28. OFS paper

29. Jacques Albert, Li-Yang Shao, and Christophe Caucheteur " Tilted fiber Bragg grating sensors" Laser and Photonics review, 7, **83,** (2013).

30. Sankhyabrata Bandyopadhyay, Tanoy Kumar Dey, Nandini Basumallick, Palas Biswas, Kamal Dasgupta, and Somnath Bandyopadhyay " High Sensitive Refractometric Sensor Using Symmetric Cladding Modes of an FBG Operating at Mode Transition" IEEE Journal of Lightwave Technol. **34**, 3348, (2016).

31. Francesco Chiavaioli, Francesco Baldini, Sara Tombelli, Cosimo Trono and Ambra Giannetti, "Biosensing with optical fiber gratings", Nanophotonics , Vol. 6, No. 4, pp. 663–679, 2017.